Predictive control approach for multicellular converters

Diego Patino, Pierre Riedinger, Claude Iung
Nancy University, Centre de Recherche en Automatique de Nancy (CRAN),
2, Avenue de la forêt de Haye
{patino.diego, pierre.riedinger, claude.iung} @ensem.inpl-nancy.fr

***Abstract*—The classic methods for controlling power converters based on average model allows a good control of the transitory state. However, the steady state (waveform, subharmonic, etc) is not always completely controlled. This article shows how to obtain an optimal periodic cycle from an average reference in currents and voltages. The optimal cycle is then used as a steady state reference for a closed loop predictive control. Moreover, the real time implementation is ensured by a neural network. Simulations and experimental results for a four-level three-cell converter verify the performance of the method.**

***Index Terms*—DC-DC power converters, hybrid systems, neural network, reference tracking.**

I. Introduction

Power converters are currently embedded in all electric devices. Their aim is to convert an electrical energy shape (voltage/current/frequency) to another one. For industrial applications with a few megawatts power, voltages in the switching components become very high (several kilovolts) and sometimes, switches cannot support these voltage values.

For surpassing this problem, a new class of power converter appeared: The multicellular converter. Studies carried out on this converter over the past ten years have shown excellent characteristics with respect to several criteria for DC/DC converters [1], [2], [3], [4].

In this article, we are interested in a four-level three-cell DC/DC converter. Its function is to split the supply voltage and to distribute it in smaller values on several levels [5], [6], [7]. Therefore, a good approximation of a particular waveform can be obtained. Fig. 1 shows a four-level, three cell converter, whose function is to feed a passive load (R-L).

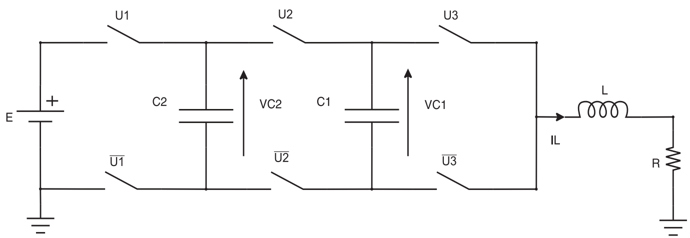

Fig. 1. Four level three cell DC/DC converter connected to an R-L load. $u_k = 1$, means that the k-th upper switch is closed and the lower switch is open ($\overline{u}_k = 0$), $k \in \{1, 2, 3\}$. $u_k = 0$, means that the k-th upper switch is open and the lower switch is closed ($\overline{u}_k = 1$)

The ability of distributing the voltage makes the control design more complex. Usually, the industry solves the problem of finding control laws, with classical control theory over the average model [8], [9], [10], [11]. Hence, neither the hybrid aspect of the system nor the high frequency are taken into account.

Another existing approach is to apply sampled linear methods with tangent approximations to the non-linear sampled model [12], [13]. In this case, the difference equation is not easily obtained and also it does not avoid high ripple between switching instants.

There are some other emerging strategies. For example, sliding modes [14], [15], predictive control [16], passivity control [17] [18] or Direct Torque Control [19]. All methods do not take into account the cyclic behavior of the system.

In this work, the problem of controlling a system with a limit cycle as steady state and whose control inputs are binary values is presented. This situation gives a good source of interesting applications, not only for three cell converter, but also for other systems whose control inputs are boolean values.

The method presented in this work shows a new approach. Firstly, we establish off-line an optimal limit cycle which is a reference cycle. Secondly, a predictive control is created in order to reach a cycle in steady state. Some simulation results of this method can be seen in [17].

The on-line implementation is ensured by an off-line training of a neural network (ANN). This network interpolates the trajectories and allows satisfying time constraints in real time. Simulations and real results show control robustness with respect to parameter variations.

The article is organized as follows: In Section 2, we present the general problem. Section 3 is devoted to open loop analysis and limit cycle research. Section 4 shows the control law in closed loop by predictive control. Section 5 shows simulation and experimental results. In section 6, some conclusions and future work are presented.

II. Problem formulation

A multicellular converter can be modelled by the following differential equation:

$$\dot{x} = f(x) + g(x)\,u \tag{1}$$

where $x \in \mathbb{R}^n$ is the state of the system, u is a boolean vector, $u \in \{0,1\}^m$. m is the number of control inputs. $f(x) \in \mathbb{R}^n$, $g(x) = [g_1(x), \ldots, g_i(x), \ldots, g_m(x)] \in \mathbb{R}^{n \times m}$, $g_i \in \mathbb{R}^n$, $i \in \overrightarrow{m} \triangleq \{1, \ldots, m\}$.

Let us assume that all the whole state in (1) is measurable.

The control problem is to find a switching law to stabilize the system in closed loop and to control x such that its average value over a period is x^{ref}.

Now, since u is an m-dimensional boolean vector, the system has 2^m possible control inputs combinations. Each combination is a mode of the system. The following definition will be helpful for the rest of the article:

Definition 1: A switching sequence is a finite set which is represented by:

$$(T, I)^s = \{(t_1, i_1), (t_2, i_2), \ldots, (t_s, i_s)\} \tag{2}$$

where

- s is the number of modes in the sequence.
- $T = \{t_1, t_2, \ldots, t_s\}$ is the time set. It indicates when a mode will be switched on.
- $I = \{i_1, i_2, \ldots, i_s\}$ is the mode set. It indicates which mode will be switched on.
- $0 \leq t_1 \leq t_2 \leq \ldots t_s \leq \infty$.
- each mode $i_j \in \{1, 2, 3, \ldots, 2^m\}$ for $j = 1, \ldots, s, s \leq \infty$.

As we already mentioned, for the power converters, the steady state is depicted by a limit cycle around an equilibrium point of the average model. Although several cycles with the same average value may exist, a cost function is able to choose only one of them. This cycle is then used as reference for the steady state.

After finding an optimal limit cycle, a tracking problem appears. Here, predictive methods can be used and control value is obtained in two ways:

- Near the optimal limit cycle produced by the sequence $(T^*, I^*)^{s^*}$: The predictive control computes only switching times T. I and s are fixed to the values I^* and s^*.
- Far from the limit cycle: T and I are optimized and the length of the sequence is fixed to s^*.

III. Steady State Determination

In order to obtain a particular waveform, a limit cycle must be chosen. The optimal cycle is produced by a sequence $(T^*, I^*)^{s^*}$. This section is devoted to determinate the time set T^*, the mode set I^* and the value of s^*, where $1 < s^* < s_{max}$.

An usual issue for power converters is the oscillations around some given reference value. Thus, a least oscillation quadratic criterion is adopted around x^{ref}:

$$J((T^*, I^*)^{s^*}) = \min_{s,I,T} \int_{t_1}^{t_f} \| x - x^{ref} \|_Q^2 \, dt \tag{3}$$

where $\| \cdot \|^2$ is a quadratic norm, Q is a weight matrix with $Q = Q^T \geq 0$, t_1 is the initial time and without loss of generality, it will be fixed to zero, $t_f = t_{s+1}$ is the final time, $x^{ref} \in \mathbb{R}^n$ is a constant reference for each state variable in (1). See Fig.2.

Remark 2: The cost function changes depending on the application. For example, for reducing the harmonic content, $J((T^*, I^*)^{s^*})$ becomes the total Distortion harmonics index.

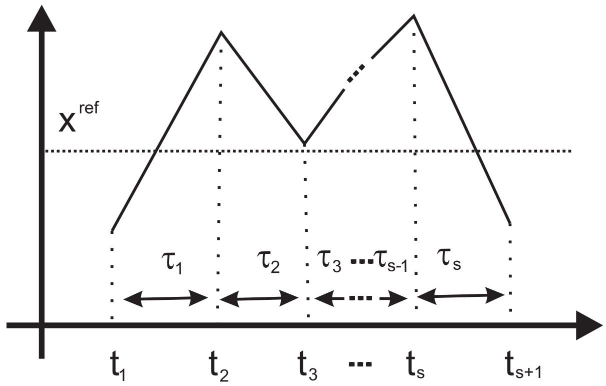

Fig. 2. Limit cycle produced by a particular sequence $(T, I)^s$ around a given reference x^{ref}

Two step summarizes the approach to determinate the solution of (3):

1) For a given s and I, the durations $\tau_j = t_{j+1} - t_j$, $j = 1, 2, \ldots, s$ are optimized with the constraints:

$$x(t_1) = x(t_f) \tag{4}$$

$$t_f = \sum_{j=1}^{s} \tau_j < T_p \tag{5}$$

$$\begin{aligned} \delta_k(t_j) \geq t_{min} |u_k(t_j) - u_k(t_{j+1})| \;\; \forall j = 1, \ldots, s \\ \dot{\delta_k}(t_j) = 1 \;\; \forall k = 1, \ldots, m \\ \delta_k(t_{j+1}) = 0 \;\; if \;\; |u_k(t_j) - u_k(t_{j+1})| \neq 0 \end{aligned} \tag{6}$$

2) The point 1 is repeated with a new I and s until all the possible sequences for $1 \leq s \leq s_{max}$ are tested.

Eq. (4) is a periodicity constraint in the state. It is a condition to obtain a periodic solution.

Eq. (5) is a constraint on the period of the cycle. T_p is an upper bound.

Eq. (6) is a boundary time condition for the switching devices. t_{min} is the dwell time for each switch. Indeed, this is the minimum allowed switching time.

δ_k is the elapsed time from the last activation of the switch k. In fact, Eq. (6) is an integrator with a reset.

It is observed that when $u_k(t_j) \neq u_k(t_{j+1})$, the switch either changes from $u_k = 1$ to $u_k = 0$ (closed $\rightarrow$ open) or from $u_k = 0$ to $u_k = 1$ (open $\rightarrow$ closed) and δ_k begins counting the time until another changes occurs. Therefore, the fist equation from (6) guarantees that the minimum switch time will be t_{min}.

Numerical algorithms can solve optimization problem (3) subject to the constraints (4)-(5)-(6). Once the solution is obtained, the sequence $(T^*, I^*)^{s^*}$ is applied to the model (1). The state evolution is considered as the reference cycle $R^{ref}(t)$ that will be used in closed loop for steady state.

We remark that instead of using the constant value x^{ref} in steady state, the choice of a cycle allows to specify a periodic steady state.

Remark 3: Since we need to solve the problem (3) $\sum_{s=1}^{s_{max}}(2^m)^s$ times, the method is numerically slow. It must be solved off-line.

IV. Closed loop construction

In this section, the closed loop elaboration is presented. The goal is to find a predictive control law which allows the system to reach the optimal limit cycle computed in the previous section.

Since the system has a fast behavior, a control law based on neural network is proposed. This controller only requires evaluation of simple functions.

For the closed loop, the length of the sequence is always fixed to the number of modes from the optimal limit cycle s^*. Fig.3, shows the structure of a neural network.

The training data for the neural network are obtained in two ways:

- Far from the limit cycle $R^{ref}(t)$. The system is in transitory state. The following cost function is minimized:
$$\min_{I,T} L(x,t) = \min_{I,T} \int_{t_1}^{t_f} \parallel x - x^{ref} \parallel_Q^2 \, dt \qquad (7)$$
The solution to (7) is obtained with respect to I and T for a given s^*. The first mode and its duration are used to train the network.
In Fig.4 the trajectory is divided in two parts according to the value of $L(x,t)$. The system is considered in transitory state when $L(x,t) > \epsilon$.
- Near the limit cycle $R^{ref}(t)$. The system is in steady state and modes I^* are known. The predictive control computes only the switching times. I and s are fixed to the reference values I^* and s^*. Thus, the cost function becomes:
$$\min_{T} \int_{t_1}^{t_f} \|x - R^{ref}\|_Q^2 dt \qquad (8)$$

For a given initial condition, all the trajectories can be founded in a given space solving (7) and (8). After generating all the trajectories, a neural network interpolates the solutions. Its principle is as follows:

1) To determinate whether the system is in transitory state or not, the value of $L(x,t)$ is checked.
2) Let ε be a vector composed by the error of each state variable $\varepsilon_h(t)$, $h = 1,\ldots,n$ with respect to the reference ($\varepsilon_h(t) = x_h(t) - R_h^{ref}(t)$ or $\varepsilon_h(t) = x_h(t) - x_h^{ref}(t)$). This vector is the input of the network.
3) When the system is in the transitory state, a solution to (7) is founded. For the steady state, we search a solution to (8).
4) An ANN interpolates the solution in a given state space to obtain an input - output function given by:
$$o_j = \Phi\left(\sum_{k=1}^{l}\left(w_{jk}\Phi\left(\sum_{h=1}^{n} v_{kh}\varepsilon_h\right)\right)\right), \; j = 1,\ldots,m+1 \qquad (9)$$
where w_{jk}, v_{kh} are the weights of the network. l is the number of neurons in the hidden layer. Eq. (9) has as input the error ε_h from the step 1. The output is the vector $o = \{o_j\} = [u^T, \tau_1]^T$, $j = 1,\ldots,m+1$ (the value of the control u and its duration). Φ is the activation function of each neuron. For more information about neural networks and training algorithms, see [20].

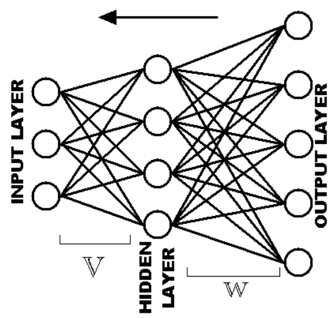

Fig. 3. A classical neuronal Network structure. The ANN interpolated open solutions in order to create a space state partition

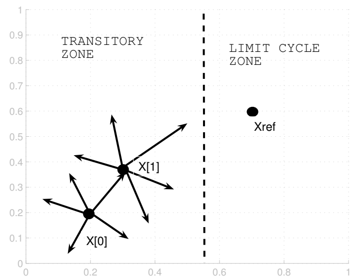

Fig. 4. From the transitory to the steady state (limit cycle). When $L(x,t) < \epsilon$, the system is in steady state. Otherwise, the system is in transitory state.

Eq. (9) gives a partition of the space (ε, u). An optimal mode is associated to each part and also a duration.

Remark 4: Since the input supply is a measurable variable, it can be added to the vector ε. Also a load estimation and the average reference value could be added as input.

V. Results

For the four level converter in the Fig. 1, V_{c1}, V_{c2} are the voltage in each capacitor. i_L is the inductance current. The state is composed by $x = [V_{c1}, V_{c2}, i_L]^T$, $m = 3$ and the functions $g(x)$ and $f(x)$ are given by:

$$g(x) = \begin{bmatrix} -\frac{i_L}{C_1} & \frac{i_L}{C_1} & 0 \\ 0 & -\frac{i_L}{C_2} & \frac{i_L}{C_2} \\ \frac{V_{C1}}{L} & \frac{V_{C2}-V_{C1}}{L} & \frac{E-V_{C2}}{L} \end{bmatrix} \qquad (10)$$
$$f(x) = \begin{bmatrix} 0 & 0 & -\frac{R}{L} i_L \end{bmatrix}^T \qquad u = \begin{bmatrix} u_1 & u_2 & u_3 \end{bmatrix}^T$$

R is the resistance, L is the inductor and E is a voltage supply. Table I gives the equivalence between modes and control values.

The first step is to solve the mathematical program (3) with constrains (4)-(5)-(6) for finding the optimal limit cycle. An

TABLE I
TABLE OF MODES

i_j	u_1	u_2	u_3
1	0	0	0
2	0	0	1
3	0	1	1
4	0	1	0
5	1	1	0
6	1	1	1
7	1	0	1
8	1	0	0

upper bound $T_p = 3ms$ is imposed. A sequence $(T, I)^*$ is searched, for $s_{max} = 12$ and

$$Q = \begin{bmatrix} 10 & 0 & 0 \\ 0 & 1 & 0 \\ 0 & 0 & 1000 \end{bmatrix}$$

The optimal sequence is:

$$\begin{aligned}(T^*, I^*)^6 = &\{(0, 2), (0.2ms, 4), (0.5ms, 7), \\ &(0.7ms, 6), (1ms, 4), (1.5ms, 7)\}\end{aligned} \quad (11)$$

It can be noticed, from Eq. (11) that the optimal period which minimizes the oscillations is 1.5 ms. It is also verified the switching constraints for $t_{min} = 1/4e3 = 0.025ms$ in each switching component.

The ANN interpolates the solution with 20 neurones in the hidden layer with a back-propagation training algorithm and sigmoid functions.

Inputs to ANN are the error ε and the voltage supply E. For better results, a load estimation and the reference value must be added to the inputs of the ANN. The parameter ϵ is equal to 0.001.

The method presented in the previous section has been validated on an experimental platform with switches MOSFET IRFP360 transistors. The parameter values are the following: $C_1 = C_2 = 45\mu F$, $R = 30\Omega$ and $L = 0.5$ H.

The voltage supply is $E = 30V$. The control objective is to hold the load current at the reference $i_L^{ref} = 0.6A$ and the capacitor voltages $V_{c_2}^{ref} = 2/3E$ and $V_{c_1}^{ref} = 1/3E$.

A few relevant performance indices were selected:

1) Start-up transient: This is a good indicator of the general performance of the controller.
2) Load transient: The load is subject to variations during operation.

Fig. 5 and Fig. 6 show the voltage V_{C1} and V_{C2} and the current i_L in a real experiment and in simulation.

Equilibrium is reached at $t = 0.04$ s without overshoot in the current. In the voltages, an overshoot is observed in the capacitor voltage V_{c1}. In V_{c2}, there is no overshoot.

Regarding the steady state, control objective is achieved considering the average values of i_L, V_{c1} and V_{c2} with a settling time of $40ms$ for the current. This is caused by the high value of the load inductance.

Fig. 7 shows the limit cycle in experiments and simulations. Fig. 8 shows the modes obtained from the neural network.

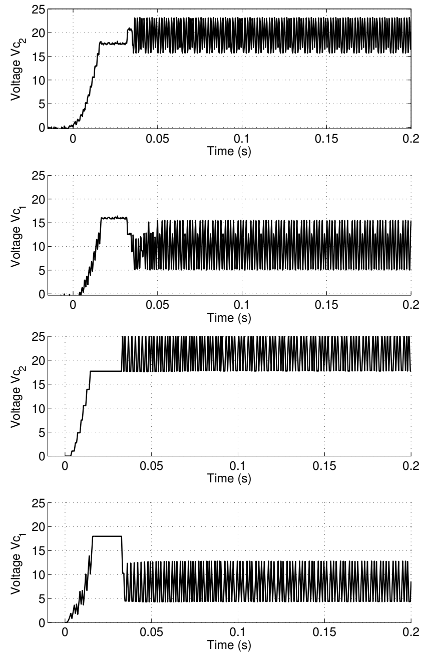

Fig. 5. Start-up transient voltage. The upper figure shows the experimental result and the lower figure the simulation result

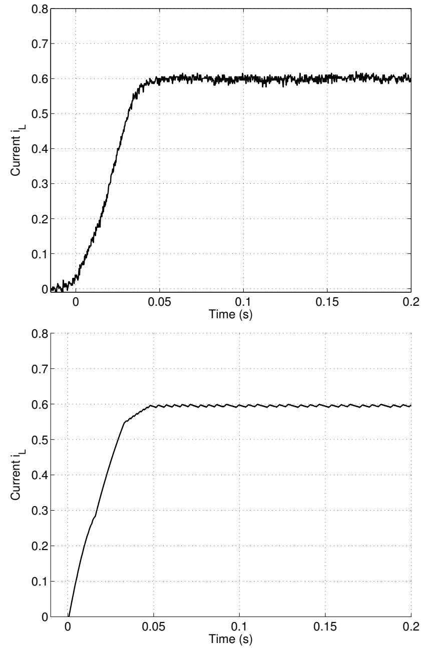

Fig. 6. Start-up transient current. The upper figure shows the experimental result and the lower figure the simulation result

The robustness with respect to the load is also verified. Figs. 9 and 10 show the converter response when a step from 20Ω to 40Ω is applied at $t = 0$. The system changes its limit cycle in 0.01s, but the regulation objective is also reached. It is also observed that the transitory in the current is different between the simulation and experimental result. It occurs because the

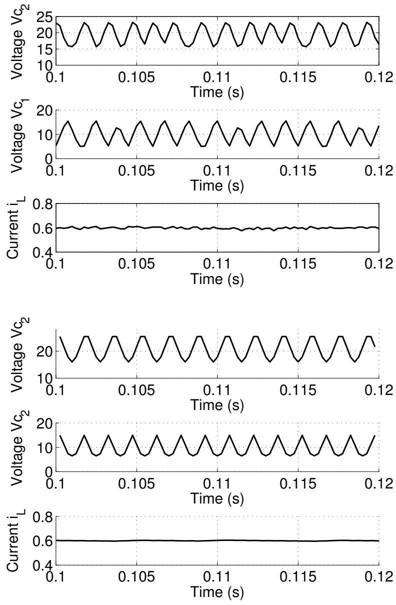

Fig. 7. Steady state voltage and current. The upper figure shows the experimental result and the lower figure the simulation result

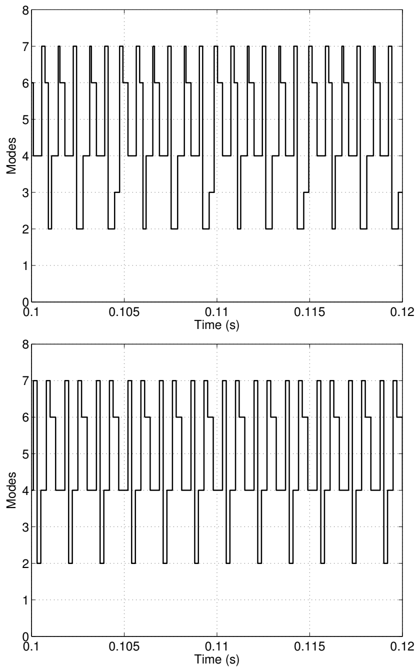

Fig. 8. Steady state control. The upper figure shows the experimental result and the lower figure the simulation result

load was changed using a manual switch and not automatically. Fig. 11 shows the current when a step in the load is applied back from 40Ω to 20Ω.

VI. Conclusions

In this work, a method for controlling a hybrid system with binary input is presented thought the important application of

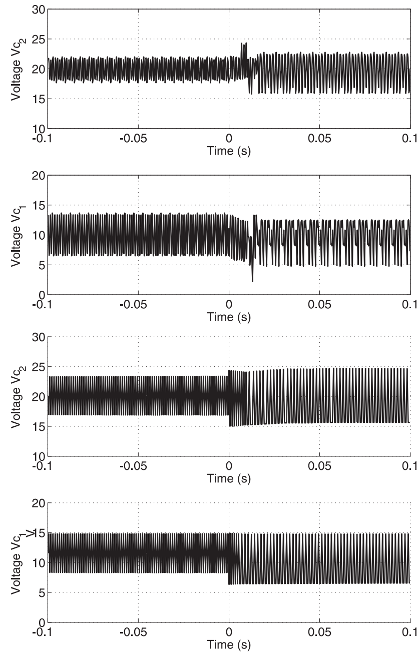

Fig. 9. Voltage response to a step in the load resistance from $R = 20\Omega$ to $R = 40\Omega$. The upper figure shows the experimental result and the lower figure the simulation result.

a four level, three cell converter.

It is composed by three parts: i) Computation of optimal limit cycle in open loop using non-linear programmation. Time constrains are included. ii) Trajectory tracking by a predictive control. iii) On-line implementation with a neural network. Indeed, the control values are obtained from the neural network output.

The method performance is shown through simulation and experimental results. It can be concluded that even if a lot of optimization algorithms are required, they are solved off-line. The method can be real implemented on very fast systems as the multicellular converter using a neural network.

In order to obtain a good operation of the converter, it is necessary to ensure the voltage balance in the cells. The results from this article shows that capacitor voltages are balanced. Therefore the performance of the control on a four level, three cell converter is verified. Moreover, voltage converge to a reference limit cycle even if there are changes in the load values.

This method can be improved by taking into account the sampling frequency in the control design. In that case, the switching times would be synchronous with the sampling period ensuring a better tracking.

In a practical point of view, the load must be considered as an unknown parameter. Thus, a load observer is necessary to guarantee the method robustness.

In this article a least oscillations criterion has been used. Nevertheless, in order to control the frequency response of the converter, a criterion with frequency aspects should be consider instead. It will be topic of future works.

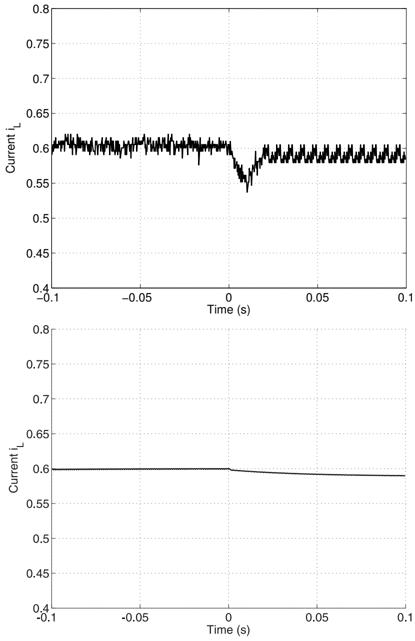

Fig. 10. Current response to a step in the load resistance from $R = 20\Omega$ to $R = 40\Omega$. The upper figure shows the experimental result and the lower figure the simulation result.

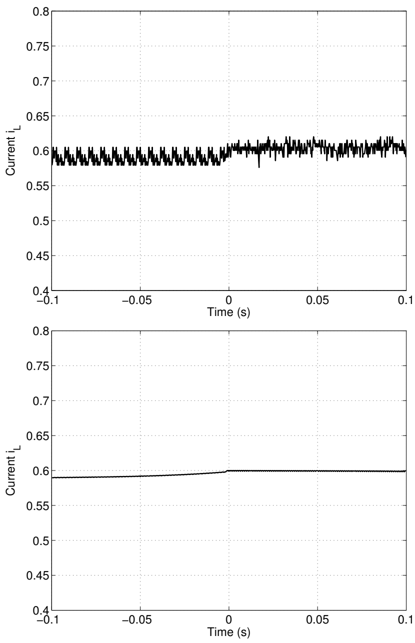

Fig. 11. Current response to a step in the load resistance from $R = 40\Omega$ to $R = 20\Omega$. The upper figure shows the experimental result and the lower figure the simulation result.

ACKNOWLEDGMENTS

- This work was supported by the European Commission research project FP6-IST-511368 *Hybrid Control (HYCON)*.
- The authors would want to thank to Mihai Baja and Hervï¿½ Cormerais from Supélec in Gif-sur-Yvette, France, for their help in the experimental results.

REFERENCES

[1] G. Gateau, G. Fades, P. Maussion, R. Bensaid, and T. A. Meynard, "Multicell converters: Active control and observation of flying capacitor voltages," *IEEE Transactions on Industrial Electronics*, vol. 49, pp. 998 – 1008, 2002.

[2] Y. Chitour, F. Jean, and E. Trélat, "Genericity results for singular trajectories," *Journal of differential Geometry*, vol. 73, no. 1, pp. 45 – 73, 2006.

[3] B. Bonnard, C. Bernard, and M. Chyba, *Singular Trajectories and their Role in Control Theory*. Series: Mathématiques et Applications, Springer SMAI, 2003.

[4] O. Béthoux and J.-P. Barbot, "Multi-cell chopper direct control law preserving optimal limit cycles," in *Proceedings of the 2002 IEEE International Conference on Control Applications*, Glasgow, 2002.

[5] T. A. Meynard, H. Foch, P. Thomas, J. Courault, R. Jakob, and M. Nahrstaedt, "Multicell converters: basic concepts and industry applications," *IEEE Transactions on Industrial Electronics*, vol. 49, pp. 955–964, october 2002.

[6] J. S. Lai and F. Z. Peng, "Multilevel converters-a new breed of power converters," *IEEE Transactions on Industrial Applications*, vol. 32, no. 3, pp. 2348 – 2356, 1996.

[7] T. A. Meynard, M. Fadel, and N. Aouda, "Modeling of multilevel converters," *IEEE Transactions on Industrial Electronics*, vol. 44, no. 3, 1997.

[8] R. Middlebrook and G. Wester, "Low-frequency characterization of switched dc dc converters," *IEEE Trans. Aerospace and Electronic Systems*, vol. AES9, 1973.

[9] R. Middlebrook and S. Cuk, "General unified approach to modelling switching dc to dc converters in discontinuous conduction mode," in *IEEE Power Electronics Specialists Conference*, 1977.

[10] S. Sanders, J. M. Noworolski, X. Z. Liu, G. C. V. Sender, and J. M. Noworolski, "Generalized averaging method for power conversion circuits," *IEEE Transactions on Power Electronics*, vol. 6, pp. 251–159, April 1991.

[11] C. Iung, J. Louis, and V. Gelezevicius, "Analysis of the validity of linear approximations for the regulation of dc motor fed by ac/dc converters," in *Proceedings of the International Conference on Electrical Machines*, Brussels, 1978.

[12] K. Mahabir, G. Verghese, and et. al., "Linear averaged and sampled data models for large signal control of high power factor converter," in *Proceedings of IEEE Power Electronics Specialists Conference*, pp. 372 – 381, 1990.

[13] F. Huliehel and S. Ben-Yaakov, "Low frequency sampled data models of switched mode dc-dc converters," *IEEE Transactions on Power Electronics*, vol. 6, pp. 55–61, 1991.

[14] A. E. Aroudi, B. Robert, and R. Leyva, "Sliding mode control of a high voltage dc-dc buck converter," in *Proceedings of the 2005 European Conference on Circuit Theory and Design*, vol. 3, pp. III/55 – III/59, 2005.

[15] D. Casini, M. Marchesoni, and L. Puglisi, "Sliding mode multilevel control for improved performances in powerconditioning systems," *IEEE Transaction on Power Electronics*, vol. 10, pp. 453 – 463, 1995.

[16] E. Silva, B. McGrath, D. Quevedo, and G. Goodwin, "Predictive control of a flying capacitor converter," in *In Proceding of IEEE American Control Conference*, (New York, USA), 2007.

[17] M. Baja, D. Patino, H. Cormerais, P. Riedinger, and J. Buisson, "Hybrid control of a four-level three-cell dc-dc converter," in *Proceedings of the 26th IEEE American Control Conference*, (New York, USA), 2007.

[18] H. Sira-Ramirez and R. Ortega, "Passivity-based controllers for the stabilization of dc-to-dc power converters," in *34th IEEE Conference On Decision and Control*, 1995.

[19] O. Béthoux and J.-P. Barbot, "Commande permettant le contrôle du convertisseur multicellulaire série à nombre non premier de cellules," in *Conférence Internationale Francophone en Automatique*, Bordeaux, France, 2006.

[20] P. Patterson, *Artificial Neural Networks*. Singapore: Prentice Hall, 1996.